FEBS Letters 585 (2011) 803–808

FEBS Letters

journal homepage: www.FEBSLetters.org

Disordered TPPP/p25 binds GTP and displays Mg^{2+}-dependent GTPase activity

Ágnes Zotter [a,1], Andrea Bodor [b,1], Judit Oláh [a], Emma Hlavanda [a], Ferenc Orosz [a], András Perczel [b,c], Judit Ovádi [a,*]

[a] Institute of Enzymology, Biological Research Center, Hungarian Academy of Sciences, H-1113 Budapest, Hungary
[b] Laboratory of Structural Chemistry and Biology, Institute of Chemistry, Eötvös Loránd University, H-1117 Budapest, Hungary
[c] Protein Modeling Group HAS-ELU, Institute of Chemistry, Eötvös Loránd University, H-1117 Budapest, Hungary

ARTICLE INFO

Article history:
Received 28 December 2010
Revised 1 February 2011
Accepted 4 February 2011
Available online 15 February 2011

Edited by Michael R. Bubb

Keywords:
Disordered protein
Tubulin Polymerization Promoting Protein/p25
GTP binding
GTP hydrolysis

ABSTRACT

The disordered Tubulin Polymerization Promoting Protein/p25 (TPPP/p25) modulates the dynamics and stability of the microtubule system and plays a crucial role in differentiation of oligodendrocytes. Here we first demonstrated by multinuclear NMR that the extended disordered segments are localized at the N- and C-terminals straddling a flexible region. We showed by affinity chromatography, fluorescence spectroscopy and circular dichroism that GTP binds to TPPP/p25 likely within the flexible region; neither positions nor intensities of the peaks in the assigned terminals were affected by GTP. In addition, we demonstrated that TPPP/p25 specifically hydrolyses GTP in an Mg^{2+}-dependent manner. The GTPase activity is comparable with the intrinsic activities of small G proteins suggesting its potential role in multiple physiological processes.

1. Introduction

The majority of intracellular proteins have well-defined secondary and tertiary structures; however, predictions based on the in silico analysis of the human genome, some of them proved experimentally, have suggested that a significant portion of the proteins does not feature predictable 3D structure [1]. These proteins denoted as *intrinsically disordered* or *unstructured* proteins contain at least one experimentally determined unstructured region [2]. Despite the lack of a well-defined structure, *intrinsically disordered* proteins and disordered regions carry out important biological functions, being typically involved in regulation, signaling and control; they seldom display intrinsic catalytic activity [1,3,4]. Their functions are linked mostly to their macromolecular assemblies, which frequently cause formation of stable aggregates. Many of them are tightly linked to the development of different neurodegenerative diseases and function as hallmark proteins [4].

Tubulin Polymerization Promoting Protein/p25 (TPPP/p25) was isolated and identified as a brain-specific protein, the primary target of which is the microtubule system [5] and it was designated as Tubulin Polymerization Promoting Protein on the basis of its in vitro and in vivo functions [6]. It is expressed endogenously mainly in oligodendrocytes; it seems to control the dynamics and stability of the microtubule system as a microtubule-associated protein [7]. TPPP/p25 expression is crucial for the differentiation of oligodendrocytes in rearrangement of the microtubule network during the projection elongation prior to the onset of myelination. In addition, we have also postulated that TPPP/p25 promotes the specific acetylation of α-tubulin affecting the microtubule-derived cell motility [8].

We have reported based on circular dichroism (CD), fluorescence spectroscopy, limited proteolysis and ^{1}H NMR studies that TPPP/p25 belongs to the family of the intrinsically disordered proteins; predictions established that the N-terminal segment of TPPP/p25 is unfolded [9,10]. More recently, multinuclear NMR studies have showed that the C-terminal part of the human paralogue TPPP3/p20, which is a truncated, N-terminal-free form of TPPP/p25, is "conformationally disordered" [11]. Previously, we showed that GTP modulates the binding of TPPP/p25 to tubulin resulting in the inhibition of TPPP/p25-induced tubulin polymerization [5]. In addition, we found that GTP suspended the influence of TPPP/p25 on microtubule-derived mitosis in *Drosophila* embryos expressing tubulin-GFP fusion protein [6].

Abbreviations: CD, circular dichroism; SDS-PAGE, sodium dodecyl sulphate–polyacrylamide gel electrophoresis; Tris, tris(hydroxymethyl)aminomethane; TPPP/p25, Tubulin Polymerization Promoting Protein/p25

* Corresponding author. Address: Institute of Enzymology, Biological Research Center, Hungarian Academy of Sciences, Karolina út 29, H-1113 Budapest, Hungary. Fax: +36 1 466 5465.
E-mail address: ovadi@enzim.hu (J. Ovádi).
[1] These authors equally contributed to the work.

0014-5793/$36.00
doi:10.1016/j.febslet.2011.02.006

In this paper we show by multinuclear NMR that the unstructured segments of TPPP/p25 are localized at the N- and C-terminal tails and straddle a flexible segment which contains potential GTP binding motifs, and that GTP, indeed, binds to TPPP/p25, which displays Mg^{2+}-dependent GTPase activity.

2. Materials and methods

2.1. TPPP/p25 purification

Human recombinant TPPP/p25 possessing a His-tag tail at N- or C-terminus was expressed in *Escherichia coli* BL21 (DE3) cells and isolated as described previously [9]. Comparative studies performed with the preparations showed virtually no difference either in the structural or in the interacting features of TPPP/p25 depending on the presence or the position of the His tag on the human recombinant protein.

2.2. Protein determination

The protein concentration was measured by the Bradford method [12] using the Bio-Rad protein assay kit.

2.3. Nucleotides

All nucleotides were purchased from Sigma–Aldrich (St. Louis, MO, USA). Nucleotide concentration was determined by UV–visible absorption spectroscopy by using the following molar extinction coefficients: for GTP and GDP $\varepsilon_{253} = 13\,700\ M^{-1}\ cm^{-1}$, and for ATP $\varepsilon_{259} = 15\,400\ M^{-1}\ cm^{-1}$.

2.4. Assignment by NMR spectroscopy

Uniformly ^{15}N-labeled TPPP/p25 was produced with the same purification procedure used for the unlabeled proteins, using M9 minimal medium containing $^{15}NH_4Cl$ as sole nitrogen source or $^{15}NH_4Cl$ and ^{13}C-glucose. Solutions containing single or double labeled TPPP/p25 (400 μM) in 50 mM tris(hydroxymethyl)aminomethane (Tris) buffer, pH 6.8 were used for backbone assignment by NMR. Spectra were acquired at 300 K using home-built 750 and 950 MHz NMR spectrometers, controlled with GE/Omega software and equipped with an Oxford Instruments Company magnet and a home-built triple-resonance pulsed-field-gradient probehead. Resonance assignments have been obtained from 3D triple-resonance HNCA, (H)CC(CO)NH NMR experiments performed on a ^{13}C, ^{15}N uniformly labeled sample. Sequential assignments were confirmed – where possible – with 3D ^{15}N-edited TOCSY-HSQC and NOESY-HSQC measurements using a ^{15}N uniformly labeled sample. GTP binding studies were performed on a Bruker DRX500 instrument equipped with a 5 mm inverse probe-head using a ^{15}N labeled sample. 2D HSQC measurements were carried out by 8 scans. All spectra were processed using the NMRPipe/nmrDraw software [13] and analyzed by CARA program, while 1D and 2D spectra visualization was achieved with TOPSPIN and with the public domain graphics program Sparky.

2.5. Affinity chromatography of TPPP/p25 on γ-amino-hexyl-GTP-Sepharose® screening column

Hundred micrograms of recombinant TPPP/p25 was applied to a 0.2 ml column of GTP-Sepharose (degree of substitution: 5 μmol GTP/ml gel) (Jena Bioscience) equilibrated with 25 mM NaCl, 20 mM Tris, pH 7.0, and the flow-through fractions (200 μl) were collected at 4 °C. The matrix was washed with an additional 0.6 ml of buffer. The retained protein was eluted with 17.4 mM, 0.4 ml of GTP solution, and fractions (200 μl) were collected. The flow-through and eluate fractions were analyzed by sodium dodecyl sulphate–polyacrylamide gel electrophoresis (SDS–PAGE), separated on a 13.5% polyacrylamide gel and stained with Coomassie Brilliant Blue R-250 containing beta-mercaptoethanol and dithioerythritol.

2.6. Fluorescence spectroscopy

Fluorescence spectra were measured on a FluoroMax-3 spectrofluorometer (Jobin Yvon Inc., Longiumeau, France), using 1 cm thermostated cuvettes at 25 °C. Scanning was repeated three times, and the spectra were averaged, the buffer spectrum was subtracted in each case. Intrinsic tryptophan fluorescence spectra of TPPP/p25 (2.4 or 8 μM) were recorded at an excitation wavelength of 290 nm (slit width 10 nm) in 10 mM Tris buffer pH 7.2. Emission spectra were collected from 300 to 400 nm (slit width 2 nm). Quenching experiments with nucleotides (MgGTP and MgATP) were performed by addition of small aliquots of concentrated stock solutions to the cuvette.

2.7. CD spectroscopy

CD spectra were acquired with a Jasco J-720 spectropolarimeter (Tokyo, Japan) in the 190–260 nm wavelength range employing 0.1 cm thermostated cuvettes at 25 °C using 20 mM Tris buffer, pH 7.2. Scanning was repeated three times at scan speed 20 nm/min with step size of 0.2 nm, and the spectra were averaged. 7.5 μM TPPP/p25 were titrated with (Mg)GTP or (Mg)ATP in the concentration range of 50–1000 μM. The reaction mixtures (200 μl) were incubated for 5 min at 25 °C before recording the spectra.

2.8. Malachite green phosphate release assay

The inorganic phosphate produced by TPPP/p25-catalyzed GTP hydrolysis was detected as described in [14]. This assay is based on quantification of the highly colored complex of phosphomolybdate and malachite green. The absorbance was measured at 660 nm by using a precision microplate reader (Wallac 1420, Perkin–Elmer). The reaction mixture containing 80 μM freshly prepared TPPP/p25 was incubated with 1500 μM nucleotide (GTP, GDP or ATP) in 20 mM Tris buffer, pH 7.4, containing 5 mM $MgCl_2$ or 5 mM Mn^{2+} or 100 mM NaCl as indicated, at room temperature. Aliquots (25 μl) were withdrawn at different incubation times and added to 100 μl of malachite green reagent to terminate the enzyme reaction. The malachite green reagent was prepared from stock solutions of ammonium molybdate (5.72%, w/v in 6 N HCl), polyvinyl alcohol (2.32%, w/v), malachite green (0.0812%, w/v), and distilled water mixed at a ratio of 1:1:2:2, respectively. Control measurements were carried out with TPPP/p25 or nucleotide solutions alone. The control MgGTP hydrolysis was subtracted from that measured in the mixture of TPPP/p25 and MgGTP. P_i calibration curve was determined with KH_2PO_4 standard.

2.9. GTP hydrolysis followed by NMR spectroscopy

Two-hundred micrograms of freshly prepared TPPP/p25 solution was typically used in 50 mM Tris buffer, pH 7.0, containing 4 mM $MgCl_2$ and 1360 μM GTP. All NMR measurements were performed at 300 K. GTPase activity was followed by ^{31}P NMR measurements at 101.25 MHz, on a Bruker Avance 250 MHz instrument, equipped with a 5 mm $^{13}C/^{19}F/^{31}P$ probe-head. 1D inverse gated ^{1}H decoupled spectra were collected using a 50 ppm spectral window, the number of scans varied between 3000–6000, a 30° pulse and a relaxation delay of 2 s was applied. The

NMR spectra in the course of GTP hydrolysis were recorded. Spectra analysis was done using the TopSpin program.

3. Results

3.1. Identification of unstructured segments of the disordered TPPP/p25

Multinuclear NMR studies were performed to identify the unstructured regions of TPPP/p25. As shown in Fig. 1A, most peaks of ^{1}H-^{15}N HSQC spectrum of the human recombinant protein are sharp and poorly dispersed in the fingerprint region. Moreover, they predominantly fall in a narrow cca 0.6 ppm ^{1}H region (7.9–8.5 ppm), a feature characteristic for intrinsically unstructured and highly dynamic proteins [15,16]. This observation supports that a large portion of the protein fluctuates among multiple conformations and lacks a well defined 3D-structure. In addition, NMR resonances of the side chain NH_2 groups (e.g., Asn, Gln) are also poorly resolved giving rise to two broad "envelopes of resonances", centered around 112 ppm (^{15}N). The lack of differentiation among these resonances suggests a broad range of exchanges happening, confirming the flexible behavior of TPPP/p25. Instead of the expected 210 backbone cross-peaks (as the 219 residue long sequence contains 9 proline residues) only about 185 are observed. The inability to detect the remaining backbone peaks may also reflect exchange broadening owing to conformational dynamics.

The analysis of the HSQC spectra showed that the intensity of the peaks is varied indicating the co-existence of disordered (high intensity resonances) and highly flexible segments (low intensity resonances). Only high intensity peaks could be assigned by using a double labeled ^{13}C-, ^{15}N-TPPP/p25 sample; on the basis of the complementary 3D HNCA and (H)CC(CO)NH measurements. The HNCA spectra gives the C^{α} resonances of the *i* and (*i-1*) residues, while the complementary measurement gives information on the chemical shifts of the (*i-1*) C spin-system, providing the chemical shift values even if the (*i-1*) residue is proline. However, due to several overlappings, not all of these intense peaks could be assigned. Based on the fact that backbone chemical shifts can be used to determine secondary structure [17], we compared the C^{α} chemical shift values of the assigned residues with the characteristic random coil values, properly corrected for the contributions by sequential neighbors. We found that this chemical shift difference has an average value of cca 0.5 ppm, situated mostly within the range of the random coil value deviation (Fig. 1B). This is the first experimental evidence for the detection of unstructured regions in TPPP/p25.

3.2. GTP binding to TPPP/p25

A representative set of GTP-binding sequence motifs (consensus sequences) was suggested by several authors for small G proteins and other GTP-binding protein families [18–20]. Our sequence alignment showed that TPPP/p25 contains four GTP binding motifs out of the five ones: three are localized within the flexible region (G^{68}-$(X)_4$GK, D^{82}-$(X)_{10}$-T, E^{46}XSAL), one (D^{181}XXG/D^{197}XXG) within the C-terminal, and one (NKXD) is missing. Thus the binding of GTP to TPPP/p25 was detected and characterized by three different approaches.

Affinity chromatography experiments showed that TPPP/p25 was retained on γ-amino-hexyl-GTP Sepharose column, and the immobilized TPPP/p25 was eluted by 17 mM GTP solution. The loaded, the unbound and bound fractions were analyzed by SDS–PAGE. As shown in Fig. 2A, virtually all loaded TPPP/p25 was immobilized onto the column and eluted with GTP solution, indicating that TPPP/p25 effectively interacts with GTP.

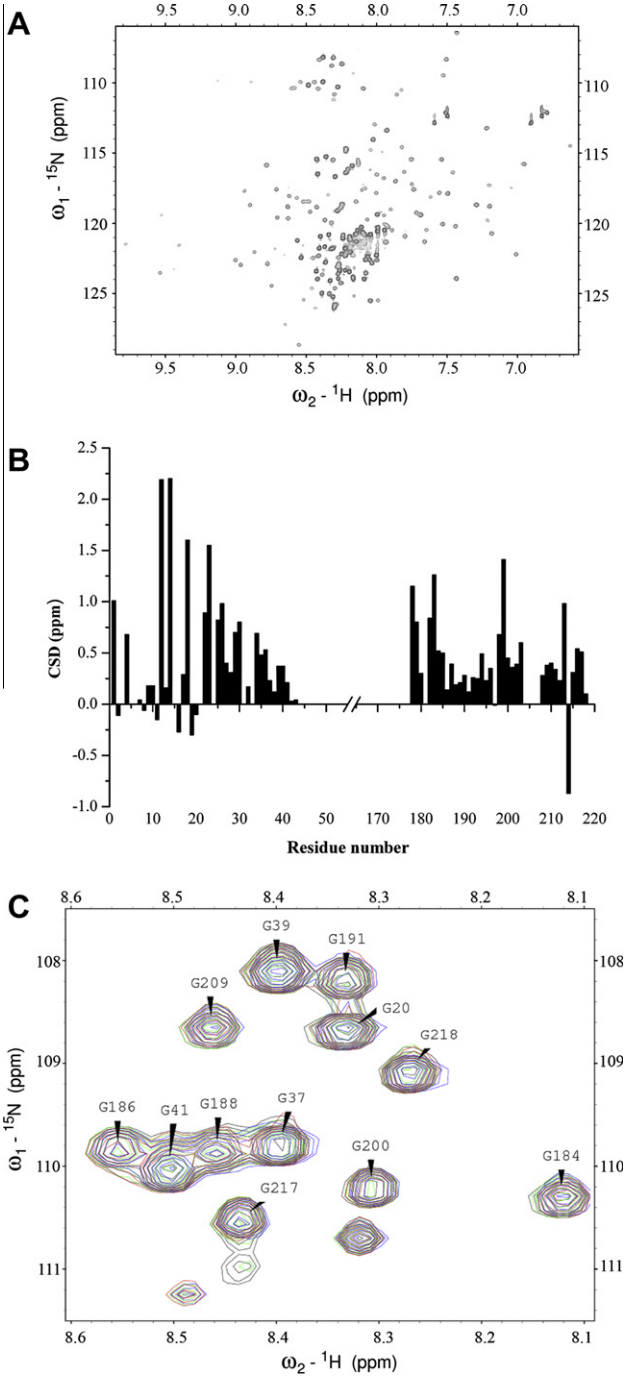

Fig. 1. NMR characterization of TPPP/p25. (A) Representative 750 MHz HSQC spectra of 400 μM ^{15}N-TPPP/p25 at 300 K. (B) C^{α} chemical shift differences (CSD) between the measured and sequence corrected random coil values in ppm for the assigned regions at the N-terminal (1–43) and C-terminal (178–219) parts. The unassigned region is omitted for clarity. (C) Overlap of HSQC spectra of 400 μM ^{15}N TPPP/25 in the absence (red) and presence (green) of 1500 μM GTP, zoomed for the glycine region.

TPPP/p25 contains a single tryptophan residue (Trp76) localized in the flexible region next to one of the GTP binding motifs. In fluorescence quenching experiments the effect of nucleotides, GTP or ATP, was tested on the intrinsic fluorescence emission of tryptophan, and as shown in Fig. 2B, GTP rather than ATP caused significant quenching in the emission of the single tryptophan residue. To correct for the increased absorption caused by the presence of nucleotides ("inner filter effect"), their effects on the fluorescence

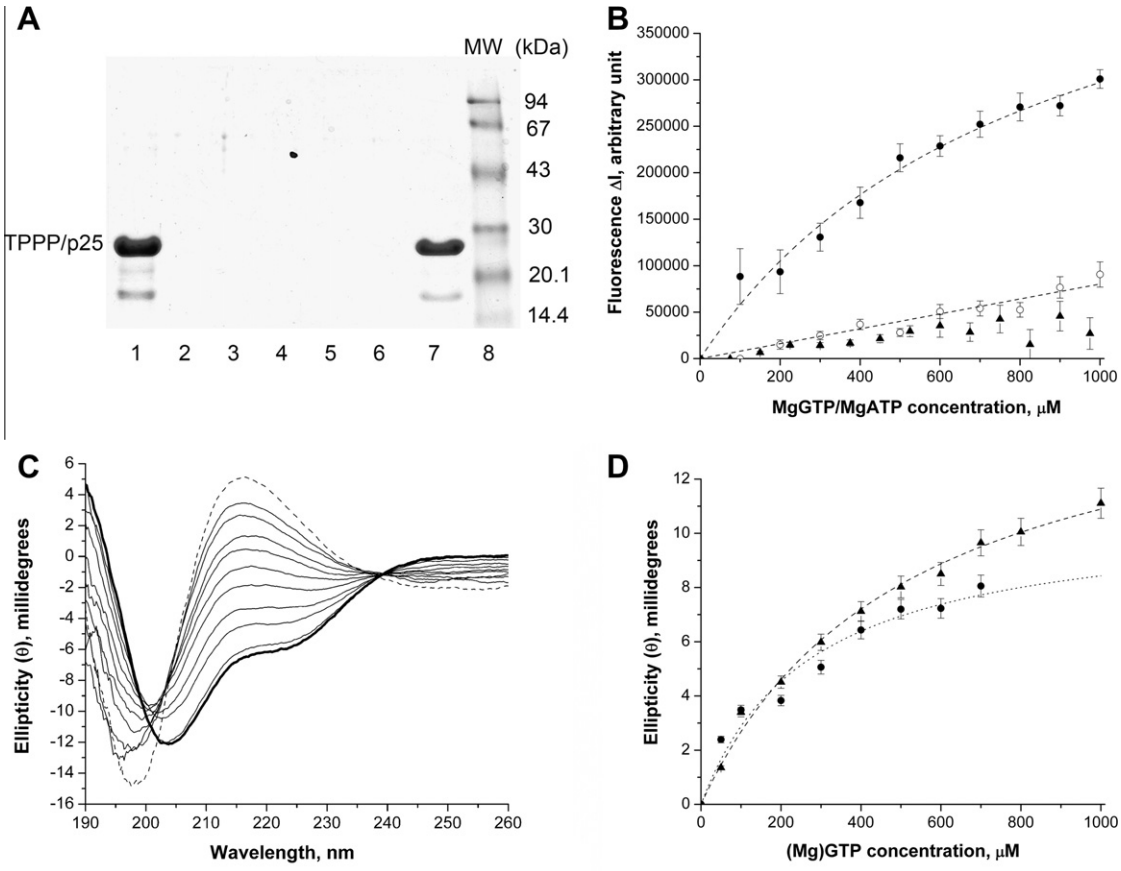

Fig. 2. Binding of nucleotides to TPPP/p25. (A) TPPP/p25 was applied to a γ-amino-hexyl-GTP-Sepharose screening column to verify the direct interaction with GTP. *Lane 1*, TPPP/p25 loaded to column; *Lane 2–5*, washing the column with buffer; *Lane 6–7*, elution with GTP; *Lane 8*, molecular weight marker. 200 μl per fraction was collected. (B) Fluorescence spectroscopy of MgGTP and MgATP binding to TPPP/p25. The fluorescence intensity difference is plotted as a function of nucleotide concentration (○: 2.4 μM TPPP/p25 and MgGTP, ●: 8 μM TPPP/p25 and MgGTP, ▲: 2.4 μM TPPP/p25 and MgATP). The average of 3 independent sets of experiments and SEM are shown. (C and D) Effects of GTP and MgGTP on the CD spectra of TPPP/p25. (C) 7.5 μM TPPP/p25 (bold line) in the absence or presence of increasing concentrations of GTP (1000 μM: dashed line), within a concentration range of 50–1000 μM (corresponding to GTP concentrations shown in Fig. 2D) in independent experiments. (D) Difference ellipticity evaluated from the CD titrations as a function of GTP/MgGTP concentrations at 205 (GTP: ▲, MgGTP: ●) nm. Difference ellipticity (in millidegrees) was calculated by subtracting the ellipticities of TPPP/p25 and MgGTP/GTP from that measured with their mixture.

emission of a model compound (N-acetyltryptophanamide) were also determined. The corrected data (Fig. 2B) showed that GTP-induced reduction in the intrinsic fluorescence of the protein is indicative for the binding of GTP to TPPP/p25, which might occur in the neighborhood of the single tryptophan.

In order to test the effect of GTP on the disordered structure of TPPP/p25, the protein was titrated with GTP or ATP, and the CD spectra were registered. The addition of nucleotides caused concentration-dependent alterations in the TPPP/p25 spectra, however, in the case of ATP, the spectrum was extensively reduced due to the inhomogeneity (turbidity) of the protein solution (data not shown). The spectral changes caused by GTP are shown in Fig. 2C. The difference spectra obtained by subtracting the ellipticities of the GTP and TPPP/p25 measured alone from that measured in the mixture of the protein and nucleotide were used to estimate IC_{50} value for the GTP binding ($IC_{50} \sim 500$ μM). As shown in Fig. 2D, Mg^{2+} increased the affinity of GTP binding.

The localization of GTP binding to TPPP/p25 was studied by HSQC spectra monitoring the changes related to the assigned peaks corresponding to backbone NH groups or their environment involved in binding. HSQC spectra of the N- and C-terminal regions in the course of GTP titration are shown in Fig. 1C, as zoomed for the Gly regions. We have found that GTP does not influence the position and intensity of the Gly peaks, nor the other peaks in the spectra of the terminal regions suggesting that they are not involved in the GTP binding. In addition, no other peaks in the spectra moved, which indirectly indicates that the highly flexible middle segment of TPPP/p25 is involved in the GTP binding.

3.3. GTP hydrolysis by TPPP/p25

In order to test whether the binding of the nucleotides to TPPP/p25 is coupled with their hydrolysis, the TPPP/p25-promoted hydrolysis of the nucleotides were measured by the malachite green phosphate release assay and by ^{31}P NMR spectroscopy. The initial assay chosen already included magnesium chloride in the reaction mixture because magnesium ions are essential for the GTPase activity for the majority of characterized GTPases ([21] and references cited therein). The assay demonstrated the time-dependent formation of P_i in the presence of 80 μM TPPP/p25, that is, TPPP/p25 exhibits hydrolytic activity towards MgGTP as shown in Fig. 3A and B. Control experiment showed that virtually no P_i release was detected in the absence of TPPP/p25 (Fig. 3B). In addition, no P_i release was detected without magnesium ions in the presence of TPPP/p25 and GTP, highlighting their crucial role for the TPPP/p25 GTPase activity. Moreover, Fig. 3A and B illustrate that significantly smaller P_i was released with either ATP or GDP even in the presence of Mg^{2+}. The GTPase activity of TPPP/p25 measured by the malachite green phosphate release assay calculated from the initial linear part of the time course is $k_{cat} = 0.018 \pm 0.001$ min^{-1}.

The measurement of the hydrolytic activity of TPPP/p25 was performed by an additional, independent method. The time course

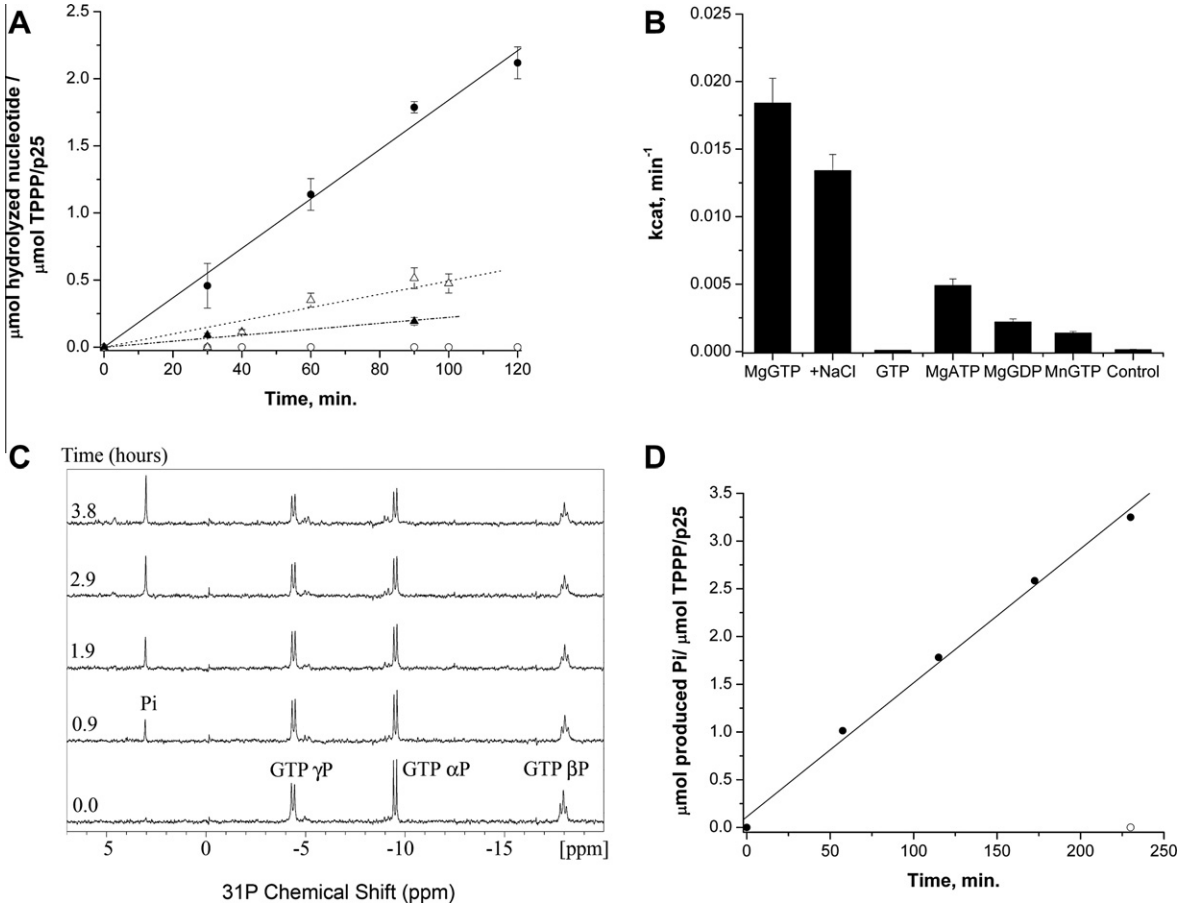

Fig. 3. GTPase activity of TPPP/p25. (A) GTPase, GDPase and ATPase activity of TPPP/p25 measured by malachite green assay in 20 mM Tris, pH 7.4 buffer containing 5 mM $MgCl_2$ or 5 mM Mn^{2+} or 5 mM $MgCl_2$ in the presence of 100 mM NaCl as indicated, nucleotide concentration was 1500 μM. (●: 80 μM TPPP/p25 + MgGTP, ○: 80 μM TPPP/p25 + GTP, Δ: 80 μM TPPP/p25 + MgATP, ▲: 80 μM TPPP/p25 + MgGDP). k_{cat} values were determined by linear fitting of the initial rates. The average of three independent sets of experiments and the SEM are shown. (B) k_{cat} values determined from the malachite green phosphate release assay. Control experiment was carried out with 1500 μM MgGTP without TPPP/p25. (C) Representative time course of GTP hydrolysis and product formation catalyzed by TPPP/p25. Reaction of 200 μM TPPP/p25, 1360 μM GTP, and 4.0 mM Mg^{2+} in 50 mM Tris buffer at pH 7.0 is monitored by ^{31}P NMR spectroscopy at 300 K. Corresponding chemical shifts in ppm are: GTP (α, β, γ): −9.52, −18.04, −4.40 and P_i: 3.08. (D) P_i production (●) as a function of the average reaction time. The P_i concentration (●) was determined from the integrated area of P_i peak. k_{cat} (0.014 min^{-1}) value was determined by linear fitting of the initial rate using the Microcal Origin version 7.0 software (Microcal Software Inc.). Control experiment, when no TPPP/p25 was added to the MgGTP, is also shown (○).

of GTP hydrolysis and P_i formation was monitored in the presence of TPPP/p25 by ^{31}P NMR spectroscopy. ^{31}P NMR spectroscopy is a straightforward tool to follow the hydrolysis of GTP both by monitoring the release of inorganic phosphate as well as the decrease of α, β and γ phosphates of GTP. The three phosphorus atoms of GTP have distinct characteristic chemical shift values: α (−9.52 ppm, doublet), β (−18.04 ppm, triplet), and γ (−4.4 ppm, doublet) and all coupling constant values are $^2J_{PP}$ = 15.8 Hz. No GTP hydrolysis was detected without the protein (Fig. 3C). As demonstrated in Fig. 3C, the addition of TPPP/p25 initiated the MgGTP hydrolysis, and the reaction was monitored by ^{31}P measurement for 4 h. The corresponding peak intensities for P_i (3.08 ppm, singlet) increased linearly until 4 h as shown in Fig. 3C and D, while the peaks of the three GTP phosphorus atoms simultaneously decreased (Fig. 4C). k_{cat} = 0.014 min^{-1} value was determined by linear fitting of the initial rate of P_i production. This finding, in concern with the results obtained by malachite green assay, shows that TPPP/p25 has inherent GTPase activity, which is specific for MgGTP.

4. Discussion

Intrinsically disordered proteins, which carry out important biological functions, can be involved in high-specificity low-affinity interactions, which render it possible their multiple binding to many partners. A number of biochemical and biophysical studies have suggested that TPPP/p25 does not have well-defined 3D structure [5–7,22]. In this work we first showed by multinuclear NMR that this protein has extended unstructured segments localized at the N- and C-terminals (45–44 aa) straddling a 130 aa flexible region. In the case of some neurological diseases the disordered proteins such as α-synuclein and tau accumulate in distinct region of the brain (inclusions) causing cell death. Makioka et al. [23] recently demonstrated that the unfolded protein response is activated in multiple system atrophy brains due to the accumulation of unfolded TPPP/p25 that we showed previously [9] emerging in the early stages of oligodendroglial

Table 1
Intrinsic GTPase activity of small G proteins.

Proteins	k_{cat} of GTPase (min^{-1})
Rac1	0.11 [27]
H-Ras	0.028 [28]
Rap1A	0.0031 [29]
Ran	0.0032 [30]
TPPP/p25	0.018/0.014 present work

pathology in this disease. This finding suggests that TPPP/p25, at least a fraction of it, could occur in unfolded state in brain tissue.

We identified by sequence alignments four of the five GTP binding motifs in TPPP/p25, three are localized in the highly flexible middle region likely responsible for the GTP binding. This recognition is based upon the indirect evidence that no chemical shift of selected glycins by addition of GTP in the assigned terminals was detected (cf. Fig. 1C). This finding is supported by the observation that the single tryptophane residue (Trp76) was quenched by GTP which is localized next to a GTP binding motif (Fig. 2B).

In this work we provide evidence for the TPPP/p25-derived GTP hydrolysis. This finding is important not merely that *a new protein could modify the nucleotide-related energy store* but perhaps more importantly that, in spite of the widespread belief, it provides experimental evidence for the catalytic function of a disordered protein. GTPase activity of TPPP/p25 was detected in the presence of magnesium ions; our results revealed that Mn^{2+} cannot replace Mg^{2+} ions (cf. Fig. 3B) which is clearly in line with the requirements of the classical GTPases [24,25].

In addition to potential role of GTP in the TPPP/p25-induced microtubule organization [6], the disordered TPPP/p25 possibly has multifarious physiological functions via its GTPase activity. We compared the activity of TPPP/p25 with that of the well-established small G proteins which typically display low intrinsic activity. We found that although the GTPase activities of the small G proteins varied in a wide range, $k_{cat} = 0.018$ and $0.014\ min^{-1}$ of TPPP/p25 obtained by two independent methods is even higher than that of some small G proteins listed in Table 1. The members of the Ras-superfamily hydrolyze GTP and act as binary switches that cycle between active (GTP-bound) and inactive (GDP-bound) states. The GTP/GDP cycle is highly regulated by specific proteins: guanine nucleotide exchange factors and GTPase activating proteins [26]. Efforts in our laboratory are in progress to identify effector molecules of TPPP/p25 which could stimulate its hydrolytic activity and may place it in the superfamily of small G proteins.

Acknowledgements

This work was supported by the Hungarian National Scientific Research Fund – OTKA (T-067963 to J. Ovádi); the European Commission (DCI-ALA/19.09.01/10/21526/245-297/ALFA 111(2010)29 to J. Ovádi); European Concerted Research Action (COST Action TD0905 to J. Ovádi), PD-76793 to J. Oláh, K72973, NK67800 and NI-68466 to A. Perczel; János Bolyai Research Scholarship of the Hungarian Academy of Sciences to J. Oláh and A. Bodor. Trans-National EC Research Infrastructure East-NMR (Contract No. 228461); Travel Grant of Boehringer Ingelheim Fonds to Á. Zotter.

References

[1] Dunker, A.K., Brown, C.J., Lawson, J.D., Iakoucheva, L.M. and Obradovic, Z. (2002) Intrinsic disorder and protein function. Biochemistry 41, 6573–6582.
[2] Sickmeier, M., Hamilton, J.A., LeGall, T., Vacic, V., Cortese, M.S., Tantos, A., Szabo, B., Tompa, P., Chen, J., Uversky, V.N., Obradovic, Z. and Dunker, A.K. (2007) DisProt: the database of disordered proteins. Nucleic Acids Res. 35 (Database issue), D786–D793.
[3] Fink, A.L. (2005) Natively unfolded proteins. Curr. Opin. Struct. Biol. 15, 35–41.
[4] Uversky, V.N. (2002) What does it mean to be natively unfolded? Eur. J. Biochem. 269, 2–12.
[5] Hlavanda, E., Kovács, J., Oláh, J., Orosz, F., Medzihradszky, K.F. and Ovádi, J. (2002) Brain-specific p25 protein binds to tubulin and microtubules and induces aberrant microtubule assemblies at substoichiometric concentrations. Biochemistry 41, 8657–8664.
[6] Tirián, L., Hlavanda, E., Oláh, J., Horváth, I., Orosz, F., Szabó, B., Kovács, J., Szabad, J. and Ovádi, J. (2003) TPPP/p25 promotes tubulin assemblies and blocks mitotic spindle formation. Proc. Natl. Acad. Sci. USA 100, 13976–13981.
[7] Ovádi, J. and Orosz, F. (2009) An unstructured protein with destructive potential: TPPP/p25 in neurodegeneration. BioEssays 31, 676–686.
[8] Tőkési, N., Lehotzky, A., Horváth, I., Szabó, B., Oláh, J., Lau, P. and Ovádi, J. (2010) TPPP/p25 promotes tubulin acetylation by inhibiting histone deacetylase 6. J. Biol. Chem. 285, 17896–17906.
[9] Kovacs, G.G., László, L., Kovács, J., Jensen, P.H., Lindersson, E., Botond, G., Molnár, T., Perczel, A., Hudecz, F., Mezo, G., Erdei, A., Tirián, L., Lehotzky, A., Gelpi, E., Budka, H. and Ovádi, J. (2004) Natively unfolded tubulin polymerization promoting protein TPPP/p25 is a common marker of alpha-synucleinopathies. Neurobiol. Dis. 17, 155–162.
[10] Orosz, F., Kovacs, G.G., Lehotzky, A., Oláh, J., Vincze, O. and Ovádi, J. (2004) TPPP/p25: from unfolded protein to misfolding disease: prediction and experiments. Biol. Cell 96, 701–711.
[11] Aramini, J.M., Rossi, P., Shastry, R., Nwosu, C., Cunningham, K., Xiao, R., Liu, J., Baran, M.C., Rajan, P.K. and Acton, T.B. (2007). Available at: <http://www.pdb.org/pdb/explore/explore.do?structureId=2JRF/>.
[12] Bradford, M.M. (1976) A rapid and sensitive method for the quantitation of microgram quantities of protein utilizing the principle of protein-dye binding. Anal. Biochem. 72, 248–254.
[13] Delaglio, F., Grzesiek, S., Vuister, G.W., Zhu, G., Pfeifer, J. and Bax, A. (1995) NMRPipe: a multidimensional spectral processing system based on UNIX pipes. J. Biomol. NMR 6, 277–293.
[14] Chan, K.M., Delfert, D. and Junger, K.D. (1986) A direct colorimetric assay for Ca^{2+}-stimulated ATPase activity. Anal. Biochem. 157, 375–380.
[15] Radhakrishnan, I., Perez-Alvarado, G.C., Parker, D., Dyson, H.J., Montminy, M.R. and Wright, P.E. (1997) Solution structure of the KIX domain of CBP bound to the transactivation domain of CREB: a model for activator:coactivator interactions. Cell 91, 741–752.
[16] Sillen, A., Barbier, P., Landrieu, I., Lefebvre, S., Wieruszeski, J.M., Leroy, A., Peyrot, V. and Lippens, G. (2007) NMR investigation of the interaction between the neuronal protein tau and the microtubules. Biochemistry 46, 3055–3064.
[17] Wishart, D.S. and Sykes, B.D. (1994) The 13C chemical-shift index: a simple method for the identification of protein secondary structure using 13C chemical-shift data. J. Biomol. NMR 4, 171–180.
[18] Dever, T.E., Glynias, M.J. and Merrick, W.C. (1987) GTP-binding domain: three consensus sequence elements with distinct spacing. Proc. Natl. Acad. Sci. USA 84, 1814–1818.
[19] Bourne, H.R., Sanders, D.A. and McCormick, F. (1991) The GTPase superfamily: conserved structure and molecular mechanism. Nature 349, 117–127.
[20] Sprang, S.R. (1997) G protein mechanisms: insights from structural analysis. Annu. Rev. Biochem. 66, 639–678.
[21] Guymer, D., Maillard, J., Agacan, M.F., Brearley, C.A. and Sargent, F. (2010) Intrinsic GTPase activity of a bacterial twin-arginine translocation proofreading chaperone induced by domain swapping. FEBS J. 277, 511–525.
[22] Hlavanda, E., Klement, E., Kókai, E., Kovács, J., Vincze, O., Tőkési, N., Orosz, F., Medzihradszky, K.F., Dombrádi, V. and Ovádi, J. (2007) Phosphorylation blocks the activity of tubulin polymerization-promoting protein (TPPP): identification of sites targeted by different kinases. J. Biol. Chem. 282, 29531–29539.
[23] Makioka, K., Yamazaki, T., Fujita, Y., Takatama, M., Nakazato, Y. and Okamoto, K. (2010) Involvement of endoplasmic reticulum stress defined by activated unfolded protein response in multiple system atrophy. J. Neurol. Sci. 297, 60–65.
[24] Zhang, B., Zhang, Y., Wang, Z. and Zheng, Y. (2000) The role of Mg^{2+} cofactor in the guanine nucleotide exchange and GTP hydrolysis reactions of Rho family GTP-binding proteins. J. Biol. Chem. 275, 25299–25307.
[25] Pai, E.F., Krengel, U., Petsko, G.A., Goody, R.S., Kabsch, W. and Wittinghofer, A. (1990) Refined crystal structure of the triphosphate conformation of H-ras p21 at 1.35 A resolution: implications for the mechanism of GTP hydrolysis. EMBO J. 9, 2351–2359.
[26] Rojas, R.J., Kimple, R.J., Rossman, K.L., Siderovski, D.P. and Sondek, J. (2003) Established and emerging fluorescence-based assays for G-protein function: Ras-superfamily GTPases. Comb. Chem. High Throughput Screen 6, 409–418.
[27] Fiegen, D., Haeusler, L.C., Blumenstein, L., Herbrand, U., Dvorsky, R., Vetter, I.R. and Ahmadian, M.R. (2004) Alternative splicing of Rac1 generates Rac1b, a self-activating GTPase. J. Biol. Chem. 279, 4743–4749.
[28] Schweins, T., Geyer, M., Scheffzek, K., Warshel, A., Kalbitzer, H.R. and Wittinghofer, A. (1995) Substrate-assisted catalysis as a mechanism for GTP hydrolysis of p21ras and other GTP-binding proteins. Nat. Struct. Biol. 2, 36–44.
[29] Hart, P.A. and Marshall, C.J. (1990) Amino acid 61 is a determinant of sensitivity of rap proteins to the ras GTPase activating protein. Oncogene 5, 1099–1101.
[30] Schweins, T., Scheffzek, K., Assheuer, R. and Wittinghofer, A. (1997) The role of the metal ion in the p21ras catalysed GTP-hydrolysis: Mn^{2+} versus Mg^{2+}. J. Mol. Biol. 266, 847–856.